



Bioconjugation of gold nanoparticles with DNA for *in situ* hybridization

Am Jang^a, Rameshwar Tatavarty^b, In S. Kim^{c,*}

^aSchool of Civil and Environmental Engineering, College of Engineering, Sungkyunkwan University, Chunchun-dong 300, Suwon, Kyonggi-do 440-746, South Korea

^bCollege of Life Sciences and Biotechnology, Korea University, Anam-dong, Seongbuk-Gu, Seoul 136-701, Republic of Korea

^cCenter for Seawater Desalination Plant, School of Environmental Science and Engineering, Gwangju Institute of Science and Technology (GIST), 261 Cheomdan-gwagiro, Buk-gu, Gwangju 500-712, Republic of Korea
Tel. +82 62 715 3381; Fax: +82 62 715 2584; email: iskim@gist.ac.kr

Received 2 May 2011; Accepted 12 March 2012

ABSTRACT

This paper examines the *in situ* hybridization (ISH) coupled with nanoparticle bioconjugates in order to address the disadvantages of using fluorescently labeled probes for ISH, as well as to access the permeability of nanoparticles across bacterial cell walls. Accordingly, relatively high hybridization temperatures are used, resulting in nanogold precipitation and leaving dark precipitated granules under the microscope. In particular, high dense black dots, representing nanogold particles sized 5–10 nm, are easily observable. Plasma membranes and cell walls measuring approximately 25 nm in thickness can also be observed within the cell. This paper specifically proves the binding of very small size (1 nm) nanogold particles exploiting streptavidin-biotin noncovalent systems. Accordingly, functionalized DNA gold nanoparticle surfaces are free to diffuse across bacterial membranes, hybridizing freely with 16s and 23s rRNA ribosomal targeted DNA. This ISH coupled with nanoparticle bioconjugates represents a beneficial tool in the detection of specific bacteria.

Keywords: Bioconjugates; Hybridization temperature; ISH; Nanoparticle; Nanogold

1. Introduction

Biofilm processes display a number of advantages for use in aquatic biosystems for water treatment. These include high concentrations of relevant organisms, resistance toward hostile environments, an increase in compact reactors, and lower sludge production. Biofilms are generally connected by various groups of micro-organisms, resulting in nonuniformity and heterogeneity. More importantly, dense microbial populations and different molecular diffusion rates generate steep substrate concentration gradients in biofilms, resulting in the creation of diffusion barriers.

Such conditions in local microenvironments may affect the population dynamics of bacteria and, consequently, alter the microbial community architecture [1]. A better understanding of the microbial compositions of biofilms is vital to improving process performance and control. For this reason, researchers have extensively examined the microbial community structures of biofilms using fluorescent *in situ* hybridization (FISH) together with imaging techniques [2–5]. However, despite such obvious utility, FISH/microscopy techniques exhibit several limitations. These limitations include overly fast photobleaching, possibly low affinity of probe-to-bacterial rRNA and signal-to-noise, as well as weak fluorescent signal strength of specific probes [5].

*Corresponding author.

Recently, many types of engineered nanomaterials, for example, TiO_2 , ZnO , fullerol, chitosan, carbon nanotubes, gold nanoparticle, silver nanoparticles, and Quantum Dots (QDs), have been utilized to increase speed, specificity, and sensitivity. Many researchers use nanoparticles functionalized with several DNA strands as sensitive and specific indicators in numerous biological processes, as well as for bioanalysis. DNA is particularly appealing due to the ease of synthesization with functional groups in desired lengths and sequences for conjugation or detection [6]. In addition, fluorescent nanoparticles, i. e. commercial QD made of CdSe, have been used as cellular labeling agents. This is due to a number of advantages such as narrow emission and broad excitation spectra, high fluorescence intensity, low photobleaching effects, long fluorescence lifetime, and high levels of resistance to chemical degradation [7]. More recently, improvements in synthetic methodologies for semiconductor QDs mean that QDs appear to be as effective as conventional fluorescent dyes in numerous biological applications [8,9]. QDs thus have tremendous potential for ISH, in which they provide common ground and means for light investigation and use in fluorescent and electron microscopic studies [10,11]. However, very few reports exist of semiconductor nanocrystals being used as active uptake mechanisms by live bacteria, in addition to their more common use as strain- and metabolism-specific labels [12,13].

The biggest challenge in applying novel nanomaterials is size. The size of nanomaterials should allow free penetration across bacterial cell walls and, after specific binding, should be able to be excluded from cells via the unbound probe. In particular, a protoplast of ~ 1 nm, a bacterial cell wall porosity (radii) of ~ 2 nm, as well as a suggested effective hole radius of 2 nm for *Escherichia coli* and 2.1 nm for *Bacillus subtilis*, have been suggested [14,15]. Some nanoparticles react with the cell walls, causing oxidative damage. In contrast, fluorescent nanocrystals can undergo deformation upon membrane binding [16,17]. The availability of the biotin group is limited after hybridization to streptavidin moieties inside tertiary structures, further adding to the complexity. Successful use of single-stranded oligonucleotide bioconjugated QDs/gold nanoparticles is very unlikely. This is because the hydrodynamic radii of these bioconjugates fall within a range of 14–50 nm, thus being unable to pass through bacterial cell walls passively. The use of streptavidin-coated gold nanoparticles (AuNP) and biotin-terminated oligonucleotide in ISH has been suggested for studies on electron microscopy studies [18]. Accordingly, this study aims to evaluate the

permeability of nanoparticles across bacterial cell walls by using ISH with nanogold-streptavidin.

2. Materials and methods

2.1. Biofilm development in a cylinder reactor

As shown in Fig. 1, biofilm was developed in an annular reactor consisting of a concentric outer cylinder (14 cm in diameter) and a rotating inner impeller with a height of 10 cm. The reactor, made of glassware, was designed for upflow operation. A continuous aerobic reactor—initially inoculated with undefined consortia of activated sludge taken from the municipal wastewater treatment plant—was used. This is done in order to develop thin biofilms on a removable tygon-plastic slide (0.8×4 cm). During cultivation, the reactor was operated in batch mode to allow for colonization and accumulation on the surfaces of disks, which were made by polymethylmethacrylate. Subsequently, the reactor was switched to continuous culture with a fresh synthetic feed solution containing 45 mg/L NH_4Cl , 100 mg/L $\text{MgSO}_4 \cdot 7\text{H}_2\text{O}$, 1,500 mg/L NaHCO_3 , 73 mg/L NaCl , and 70 mg/L K_2HPO_4 , as well as a trace mineral solution, for 5 h of hydraulic residence time (HRT). Biofilms were cultured in a substrate solution with little or no carbon traces in order to minimize heterotrophic bacterial growth. During experimental operation, the culture temperature and pH were kept at 20 ± 1 and $7.5 \pm 0.2^\circ\text{C}$, respectively. Eight removable slides—offering surfaces that could be easily sampled for biofilm growth—were carefully removed from each disk once every five days.

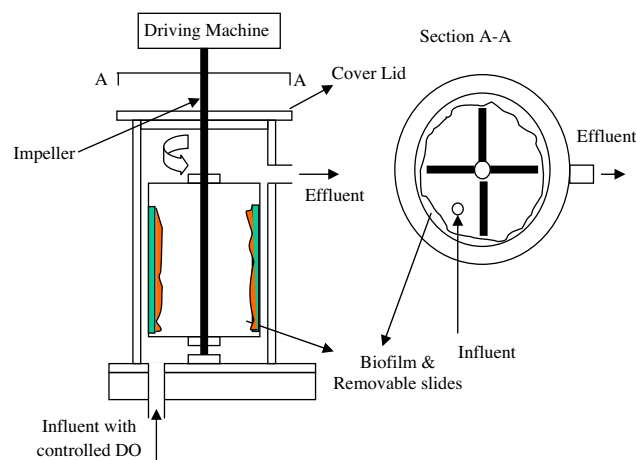


Fig. 1. Schematic diagram of annular reactor (reactor volume: 1899.7 cm^3 , wetted surface area: 78.5 cm^2 , reactor height and diameter: 20, 11 cm, inside height and diameter: 12, 10 cm, flow rate: 100 mL/min, HRT: 9.42 min, pH: 7.6, temperature: 22°C , impeller peripheral velocity: 15 cm/s).

2.2. FISH for biofilms

Cell fixation was used to kill cells and preserve the target RNA and DNA from endogenous nucleases. Following this, the majority of cells were permeable by single-stranded and short oligonucleotide probes labeled with fluorescent dye. The excess probe was washed after hybridization and visualized by a confocal laser scanning microscope (CLSM) (Carl Zeiss, Germany) equipped with Zeiss filter sets 09 and 15, as well as an Ar-ion laser (488 nm). In addition, a He-Ne laser (543 nm) was used to record optical sections of the biofilm specimen. For reference, the details of fixation and hybridization were described in a previous publication [1].

2.3. ISH procedures and observations

2.3.1. Cell growth and fixation

The bacteria *E. coli* (KCCM 12,119, gamma proteobacteria) and *Paracoccus denitrificans* (ATCC 13,543, alpha proteobacteria) were grown on a medium nutrient broth (234,000, Difco) under standard aerobic conditions in a shaking incubator at 35°C for 24 h. Further, 1 mL of culture broth was centrifuged at 10,000 rpm for 3 min at room temperature. The supernatant was removed, and 1 mL of 1× phosphate-buffered saline (PBS) pH 7.2 (PBS: 130 mM NaCl, 7 mM Na₂HPO₄, 30 mM NaH₂PO₄) was added for washing, being resuspended, and centrifuged again at 10,000 rpm for 3 min. Following removal of the supernatant, the washed cell mass was fixed in 1 mL of 4% paraformaldehyde. Fixation was executed at 4°C in the dark for 3 h. Upon successful fixation, the mass was centrifuged at 14,000 rpm for 3 min and twice washed with 1 mL of 1× PBS.

2.3.2. Preparation of fixed cells for hybridization

Initially, 10 µL of fixed *E. coli* cells was spotted on poly-L-lysine-coated slides (LabScientific, Inc.). Subsequently, the sample slide was dried for 5 min at 35°C and dehydrated by sequentially dipping the slides for 3 min in 50, 80, and 96% ethanol:water mixtures. Finally, the slides were dried at 35°C for 3 min, being again used in hybridization experiments.

2.3.3. Bacterial ISH with nanogold-streptavidin and silver enhancement

A GAM42a probe was commercially synthesized (Genotech, Korea) with a 5′-GCC TTC CCA CAT CGT TT-3′ sequence tagged with a 5′-biotin molecule. For

hybridization, 40 µL of a biotinylated oligonucleotide GAM42a probe (80 µg/mL) was added to 360 µL of a preheated hybridization buffer (0.9 M NaCl, 0.1% SDS, 20 mM Tris-HCl, and formamide 40% (v/v)), (hybridization buffer:probe ratio 9:1, v/v) and slightly mixed viagentle stirring with a pipette. The GAM42a represented a phylogenetic oligonucleotide probe for gamma proteobacteria with a target molecule of 23s rRNA. The biotinylated GAM42a probe and hybridization buffer mixture were applied to the slide and sealed with Secure-Seal™ hybridization chambers (Grace Bio-labs, USA), being incubated at 48°C for 3–16 h in a rotating hybridization oven. Following hybridization, the slide was briefly rinsed with distilled water and then treated with 400 µL of a prewarmed washing buffer (80 mM NaCl, 20 mM Tris-HCl, 0.1% SDS, pH 7.2) for 20 min at 46°C to reduce toxic waste and to remove the unbound probe. Upon removal of the washing buffer, 400 µL of streptavidin-Nanogold® (Nanoprobes Inc., USA) diluted to 1:100 in PBS was added to the slide and incubated at RT for 2 h. The sample was then washed twice in PBS containing 0.1% gelatin, before being repeatedly washed in distilled water for at least 10 min.

Finally, the sample was rinsed twice in ultrapure water (EM-grade). Sterile and disposable containers were used to ensure that the sample was clean and free of all salts and metal ions. For solution A, 40 mg of silver acetate (code 85140; Fluka, Buchs, Switzerland) was dissolved in 20 mL of distilled water. Silver acetate crystals were dissolved by stirring continuously for 15 min. For solution B, 100 mg of hydroquinone (15,616, Riedel-de Haen) was dissolved in 20 mL of citrate buffer. The citrate buffer was made of 23.5 g of trisodium citrate dihydrate (S-4641, Sigma) and 25.5 g of citric acid monohydrate (251275, Sigma) in 850 mL of distilled water. This was then adjusted to a pH of 3.8 using a citric acid solution. The sample slides were dipped vertically in a 50-mL conical tube containing a 40-mL mixture of solutions A and B. These solutions A and B were freshly prepared for every run and were mixed together immediately prior to use; staining occurred over a 5–10 min period. Once silver development was completed, the slides were rinsed twice in distilled water. Next, the slides were soaked as follows: in distilled water for 3 min, in 50% alcohol for 1 min, in 80% alcohol for 1 min, and in 96% alcohol for 1 min.

2.3.4. Light microscopy, TEM, and SEM observations

Finally, the slide—on which *E. coli* was both hybridized *in situ* with nanogold-streptavidin and

silver-stained—was washed twice with ultrapure water and dried in the dark. One drop of mounting solution (M1289, Sigma) was placed on the dried sample slide. The coverslip was then placed on the slide without air bubbles and sealed with nail polish. Light microscopy observations were performed with an inverted LSM5 confocal laser scanning microscope (Zeiss, Germany). This process makes use of the Plan-Neofluar 100 \times /1.3 oil and C-Apochromat 63 \times /1.2 w objective.

All samples of ISH cells were prepared for observation via transmission electron microscopy (TEM) according to similar procedures related to biological sample fixing and embedding [19]. Approximately 107–108 *E. coli* cells were fixed for 2 h in 4% paraformaldehyde and 1% glutaraldehyde in a 0.1 M phosphate buffer (pH 7.4) by mixing an equal volume of fixative and cell suspension. Upon removal of the fixative cells, the remaining cells were postfixed in buffered 1% OsO₄ at 40°C for 1 h. Following this, cell dehydration was conducted in a higher concentration of an ethanol:water mixture (50>70>90>100%). The cell pellet embedded in EPON resin was allowed to polymerize. Samples were then cut with a diamond knife in 50–100-nm thick slices, deposited on bare 200 mesh copper grids, and stained with 2 wt.% uranyl acetate, followed by 2 wt.% lead citrate, for 5 min each. Finally, the sectioned grids were washed twice with ultrapure water. The grids were dried in a vacuum oven overnight and examined using a Carl Zeiss EF-TEM Leo 912AB at 120 kV. For pure gold particles, 5 μ L of a 10⁻¹ diluted 0.01 mM colloidal gold solution was spotted, dried, and observed on a copper grid using a Philips FE-TEM electron microscope operating at 200 kV.

Scanning electron microscope (SEM) studies were carried out on hybridized cells to detect any nonspecific binding on bacterial cell walls. This was done using a Hitachi 4,700 microscope (15 kV) equipped with an EMAX (Energy-Dispersive Micro-Analysis of X-ray) SEM. The glass slides were dried in a vacuum oven for 6 h after hybridization. An area of hybridized cells was then carefully cut into approximately square pieces with a slide length of 0.5 mm. Specimens were taken from ethanol and placed in amyl acetate, being critical point dried with liquid CO₂. Dried specimens were carbon-coated with 10-nm thick gold using a SEM turbo carbon coater (AGAR Scientific Elektron Technology UK Ltd.) for SEM observations.

2.4. Nanogold and streptavidin

Nanogold–streptavidin (80 μ g/mL) was stored in 20 mM PBS (150 mM NaCl) at pH 7.4, with 0.1%

bovine serum albumin and 0.05% sodium azide. Nanogold–streptavidin particle sizes were seen to be uniform with 1.4-nm diameter gold particles (\pm 10%), being chromatographically purified through gel filtration columns. The stoichiometry of streptavidin—in relation to gold particles—was one, and experimental conditions did not exceed 50°C. Further, particles were stable within a wide range of pHs and ionic strengths for hybridization experiments. For reference purposes, more detailed information can be found in additional literature [20].

3. Results and discussion

3.1. Biofilm development

Biofilm thickness is nearly constant at 80–170 μ m in a steady state when the ammonium ion-loading rate was 1.2 g NH₄⁺/m²/day. As the biofilm grew, stable nitrification was obtained 14 days after continuous feed of the synthetic solution. The bacterial population was seen to increase noticeably as time passed. The removal efficiency of ammonium ion persisted at over 95%, while effluent ammonia concentration averaged less than 2.0 mg NH₄⁺/L. In addition, nitrate concentration in the bulk solution increased exponentially as the biofilm thickened, reaching a steady state after approximately 14 days. Such results indicated that

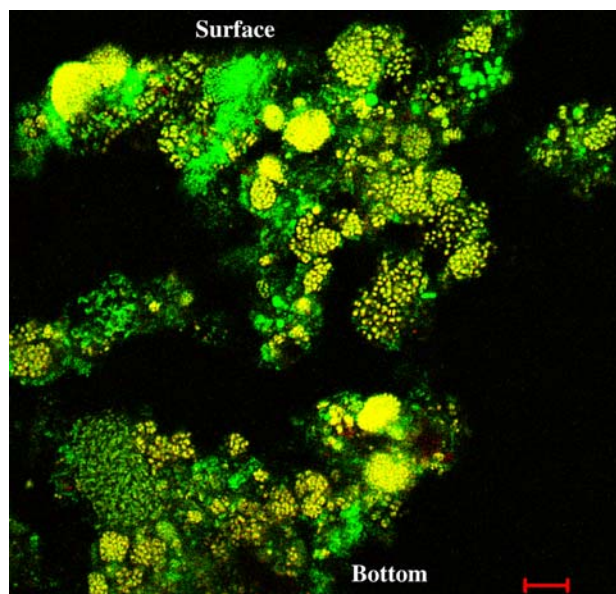


Fig. 2. Development of AOB populations in artificially cultured biofilms after *in situ* double hybridization with FITC-labeled probe EUB338 and TRITC-labeled probe Nso190 under condition of 45 mg NH₄⁺/L. AOB is visualized in yellow due to binding of both probes such as EUB338 (green) and Nso190 (red). The inset shows a large aggregate hybridized with upper probes; scale bar is 20 μ m and magnification 400 \times .

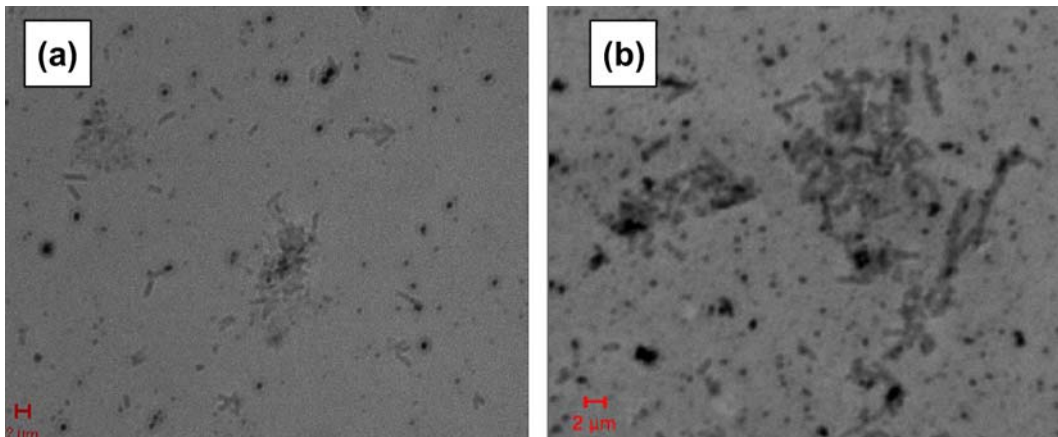


Fig. 3. Initial optimization experiments for nanogold-ISH and light microscopic observations.

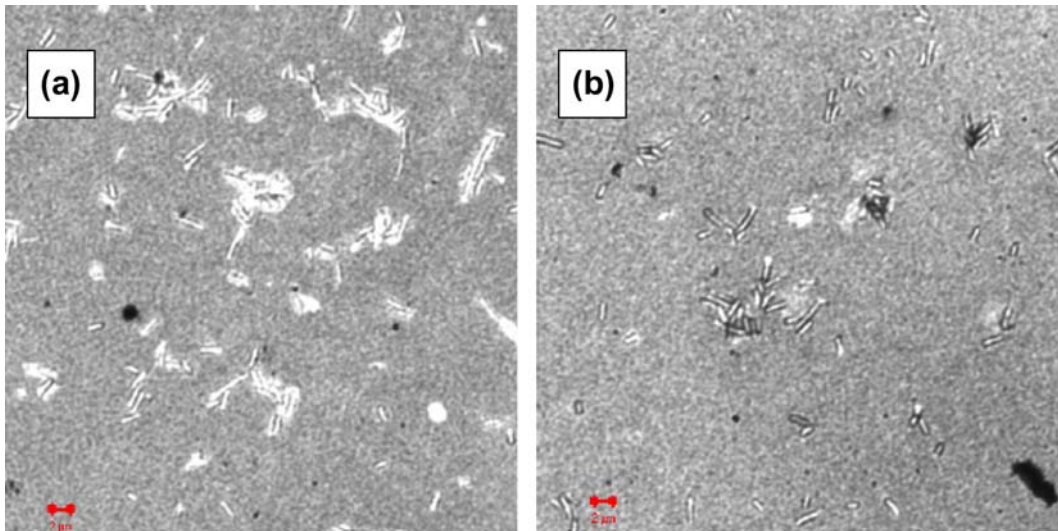


Fig. 4. The ISH hybridization of *E. coli* cells after silver enhancement. (a) *E. coli* cells hybridized by an unlabeled GAM42a probe and (b) *E. coli* cells labeled with a biotinylated GAM42a probe; the hybridized cells show the highest contrast on the cell wall.

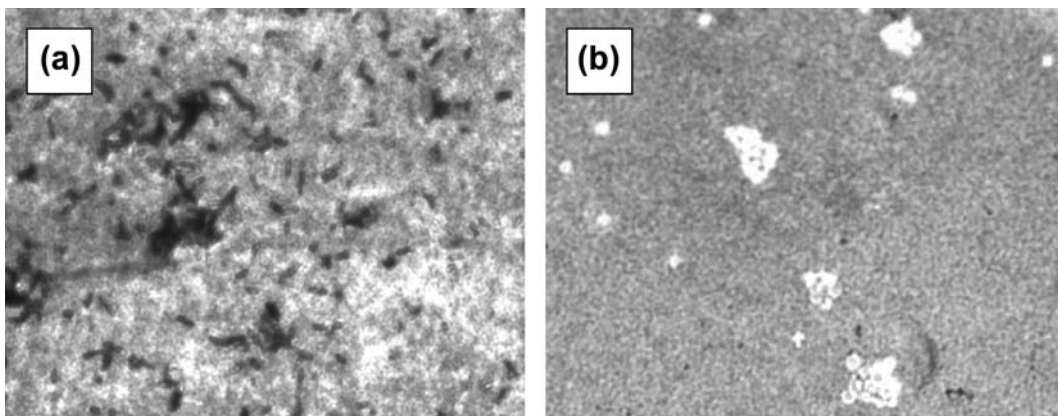


Fig. 5. Light microscopic ISH images of (a) *E. coli* cells and (b) *P. denitrificans* cells (magnification 65 \times).

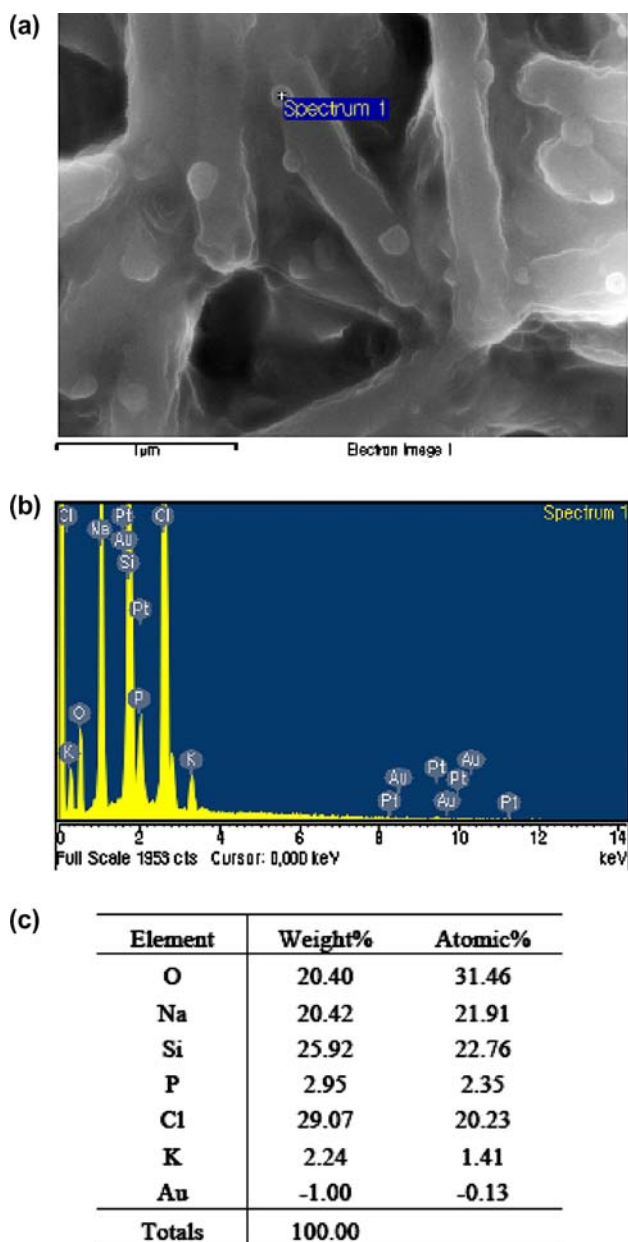


Fig. 6. SEM observation showing (a) *E. coli* cells, (b) EMAX result of granules on the bacterial cell surface, and (c) components of granules obtained from EMAX.

bacterial settlement occurred on slide coupons after 14 days. After two weeks of operation, reactor biofilms grown on slides were seen to be darker, smoother, and thicker than biofilms obtained before the 14-day period. Further, such biofilms displayed higher cell density and were nonuniformly distributed on slides. The biofilms developed on slide coupons before the 14-day period were used for studying biofilm structures, as well as identifying ammonium oxidizing bacteria (AOB) using FISH with CLSM.

3.2. Monitoring of biofilm structure using FISH

FISH 190 was carried out with specific probes such as NEU and N so for all vertical sections of biofilm in order to investigate the spatial distributions of AOB within biofilms. Microslicing combined with FISH allowed for AOB detection of biofilm on the slides. Cryosectioning, i.e. cutting sections from frozen material, can be performed in vertical or horizontal directions. As shown in Fig. 2, small amounts of AOB were found on the surface of nearly all slides, since oxygen appears insufficient at deeper layers of biofilm. In other words, AOB can be detected primarily in the upper and middle layers of the biofilms due to deficient oxygen transfer. Oxygen concentration can thus be regarded as a vital factor specifically affecting the AOB growth rate.

In spite of intensive research, individual cells non-uniformly distributed within the biofilms were not easily distinguishable. This was because the majority of AOB seemed to form dense spherical microcolonies. A variety of eubacteria—detected with a general bacterial probe, EUB 338—surrounded and coexisted with AOB. Sensitivity strongly decreased as a result of unspecific probe attachment of sludge flocs, as well as interference of naturally occurring activated sludge microbiota in flocs. In addition—since fluorescence signals may be influenced by a whole range of factors, both external and intrinsic to fluorescence—misidentification and the possibility of overlooking fluorescent signals of the probe vis-a-vis brighter backgrounds may obviously represent a many serious drawback for FISH detection [21].

In order to ensure high magnification and resolution, ISH—coupled with nanogold streptavidin—was tested. Streptavidin-coated nanogold was used to detect biotinylated oligonucleotide ISH probes inside the bacteria. Ultrathin 2-g sections of bacterial-negative species were tested for positive and false positive results through TEM observation. In addition, optical light microscopy was used to determine differentiation. Many different media exist with which to perform ISH, for example in liquid, on membrane surfaces, even on adhesive tapes. However, the most satisfactory results observed with free floating cells were achieved with direct placement in a hybridization solution. Contrast was greatly enhanced through the use of sealants on glass slides, resulting in effective hybridization. The use of higher hybridization temperatures resulted in the precipitation of nanogold, leaving dark precipitated granules when viewed under a microscope. Therefore, hybridization temperatures were determined to be ideal below 55°C. Further, the length of hybridization affected hybridization more than conventional FISH; in particular, the length of hybridization led to higher contrast during optical

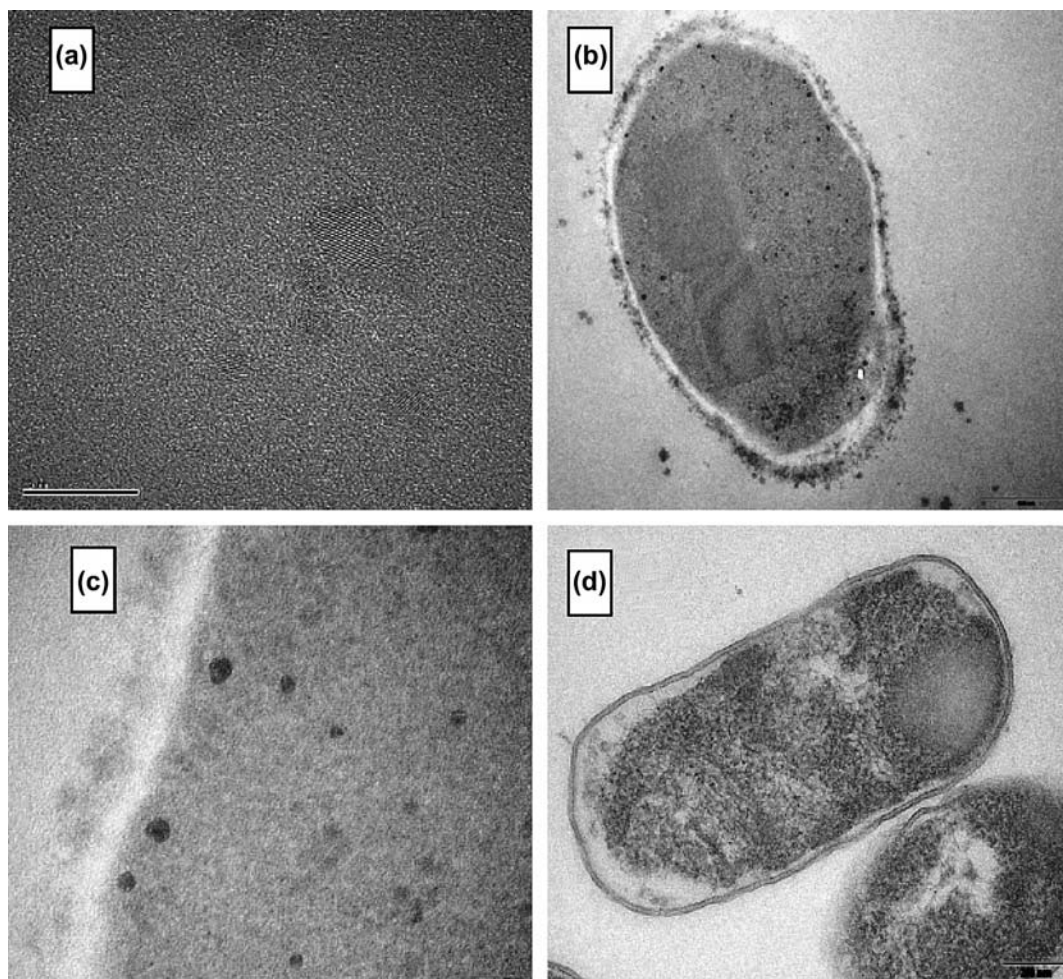


Fig. 7. TEM observation of (a) core of bare nanogold particles (scale 10 nm), (b) TEM image of a cross-sectional view of *E. coli* cells showing nanogold particles inside the cells (scale 500 nm), (c) TEM image of cross-sectional view of *E. coli* under higher magnification showing nanoparticles inside the cell wall (scale 50 nm), and (d) TEM image of cross-sectional view of *E. coli* cell in which no nonspecific binding is detected (scale 200 nm).

observation. For each optimization step, negative controls were also kept. *E. coli* cells were also hybridized without biotin moiety, using only a GAM42a probe. These cells revealed no contrast compared with *E. coli* cells hybridized with a biotinylated GAM42a probe, as shown in Fig. 3. Using a microscope without silver enhancement, increased contrast maybe easily differentiated. Moreover, digital images were recorded by keeping all parameters of the microscope and digital camera identical.

Fig. 4 represents the same experimental condition, but includes the additional step of silver enhancement. Although contrast was seen to increase, additional precipitation of black metallic silver was observed on the glass slides. Further, a relative increase of metal ion precipitation was observed on the glass slide in which biotin moiety was used with the oligonucleotide probe.

Despite the fact that the ISH of *E. coli* were tested against *P. denitrificans*—belonging to an alpha-subgroup of proteobacteria—the *E. coli* cells were hybridized not as a mixture, but on different glass slides for the sake of clarity. Such bacteria do not normally hybridize to a GAM42a probe, therefore serving as a negative control for specificity. Fig. 5 displays a higher contrast under a bright-field microscope, in which *E. coli* cells can be clearly observed in a dark contrast compared with *P. denitrificans* cells.

3.3. SEM observations

The nonspecific binding of probes to the sample may possibly lead to a false result. Thus, SEM observation was conducted to determine the nonspecific binding of nanogold particles on cell surfaces of stained *E. coli* cells. EMAX results indicate no presence of gold or silver

elements, despite the fact that some granules are observed on the cell surface, as shown in Fig. 6.

3.4. TEM images of *in situ* hybridization with nanogold particles

Fig. 6(a) illustrates the core size of nanogold particles used in the study. Fig. 7(b) shows clear binding of nanogold particles inside an *E. coli* bacterial cell wall. Highly dense black dots, representing nanogold particles of 5–10 nm in size, can be easily seen. Fig. 7(c) displays the high magnification image. Moreover, the plasma membrane and cell wall, representing a thickness of approximately 25 nm within the cell, may also be observed in both Fig. 7(b) and (c). Fig. 7(d) depicts a cross-sectional view of *E. coli* cells, revealing an absence of nanogold particles.

4. Conclusions

This paper executes an optical FISH method for AOB monitoring during nitrification. Stable nitrification is seen to occur via the formation of thin nitrifying biofilm enriched with AOB. According to molecular FISH and CLSM, fluorescence may be concluded as being a reliable indicator of AOB. In addition, this study proves that very small size nanogold particles exploiting the streptavidin–biotin noncovalent system are able to bind specifically. Such results indicate that the surfaces of functionalized DNA gold nanoparticles are free to diffuse across bacterial membrane, being able to hybridize freely with 16s ribosomal targeted DNA. In conclusion, such a method could prove to be a very beneficial tool in the detection of specific bacteria.

Acknowledgments

This research was supported by a Grant (07SeaHeroA01-01) from Plant Technology Advancement Program funded by Ministry of Land, Transport and Maritime Affairs, and in part by the National Research Foundation of Korea (NRF) grant funded by the Korea government (MEST) (2011-0006866).

References

- [1] A. Jang, S. Okabe, Y. Watanabe, I.S. Kim, P.L. Bishop, Measurement of growth rate of ammonia oxidizing bacteria in partially submerged rotating biological contactor by fluorescent *in situ* hybridization (FISH), *J. Environ. Eng. Sci.* 4 (2005) 413–420.
- [2] A. Jang, W.T. Kim, I.S. Kim, Simultaneous removal of volatile organic compounds (VOCs) and nitrogen: batch test, *J. Environ. Sci. Health A: Tox./Hazard. Subst. Environ. Eng.* 38 (2003) 2955–2966.
- [3] A. Jang, Y.H. Yoon, I.S. Kim, K.S. Kim, P.L. Bishop, Characterization and evaluation of aerobic granules in sequencing batch reactor, *J. Biotechnol.* 105 (2003) 71–82.
- [4] A. Terada, S. Lackner, K. Kristensen, B.F. Smets, Inoculum effects on community composition and nitrification performance of autotrophic nitrifying biofilm reactors with counter-diffusion geometry, *Environ. Microbiol.* 12 (2010) 2858–2872.
- [5] A. Woznica, A. Nowak, C. Beimfohr, J. Karczewski, T. Bernas, Monitoring structure and activity of nitrifying bacterial biofilm in an automatic bioreactor of water toxicity, *Chemosphere* 78 (2010) 1121–1128.
- [6] L.M. Dillenback, G.P. Goodrich, C.D. Keating, Temperature-programmed assembly of DNA: Au nanoparticle bioconjugates, *Nano Lett.* 6 (2006) 16–23.
- [7] X. Wang, X.H. Lou, Y. Wang, Q.C. Guo, Z. Fang, X.H. Zhong, H.J. Mao, Q.H. Jin, L. Wu, H. Zhao, J.L. Zhao, QDs-DNA nanosensor for the detection of hepatitis B virus DNA and the single-base mutants, *Biosens. Bioelectron.* 25 (2010) 1934–1940.
- [8] X.H. Gao, L.L. Yang, J.A. Petros, F.F. Marshal, J.W. Simons, S. M. Nie, *In vivo* molecular and cellular imaging with quantum dots, *Curr. Opin. Biotechnol.* 16 (2005) 63–72.
- [9] J.K. Jaiswal, H. Mattoussi, J.M. Mauro, S.M. Simon, Long-term multiple color imaging of live cells using quantum dot bioconjugates, *Nat. Biotechnol.* 21 (2003) 47–51.
- [10] R. Tubbs, J. Pettay, M. Skacel, R. Powell, M. Stoler, P. Roche, J. Hainfeld, Gold-facilitated *in situ* hybridization—a bright-field autometallographic alternative to fluorescence *in situ* hybridization for detection of HER-2/neu gene amplification, *Am. J. Pathol.* 160 (2002) 1589–1595.
- [11] E. Gerard, F. Guyot, P. Philippot, P. Lopez-Garcia, Fluorescence *in situ* hybridisation coupled to ultra small immunogold detection to identify prokaryotic cells using transmission and scanning electron microscopy, *J. Microbiol. Meth.* 63 (2005) 20–28.
- [12] J.A. Kloepfer, R.E. Mielke, M.S. Wong, K.H. Nealson, G. Stucky, J.L. Nadeau, Quantum dots as strain- and metabolism-specific microbiological labels, *Appl. Environ. Microb.* 69 (2003) 4205–4213.
- [13] J.A. Kloepfer, R.E. Mielke, J.L. Nadeau, Uptake of CdSe and CdSe/ZnS quantum dots into bacteria via purine-dependent mechanisms, *Appl. Environ. Microb.* 71 (2005) 2548–2557.
- [14] R. Scherrer, P. Gerhardt, Molecular sieving by the *Bacillus megaterium* cell wall and protoplast, *J. Bacteriol.* 107 (1971) 718–735.
- [15] P. Demchick, A.L. Koch, The permeability of the wall fabric of *Escherichia coli* and *Bacillus subtilis*, *J. Bacteriol.* 178 (1996) 768–773.
- [16] P.K. Stoimenov, R.L. Klinger, G.L. Marchin, K.J. Klabunde, Metal oxide nanoparticles as bactericidal agents, *Langmuir* 18 (2002) 6679–6686.
- [17] S. Dwarakanath, J.G. Bruno, A. Shastry, T. Phillips, A. John, A. Kumar, L.D. Stephenson, Quantum dot-antibody and aptamer conjugates shift fluorescence upon binding bacteria, *Biochem. Biophys. Res. Commun.* 325 (2004) 739–743.
- [18] T. Kenzaka, A. Ishidoshio, N. Yamaguchi, K. Tani, M. Nasu, RRNA sequence-based scanning electron microscopic detection of bacteria, *Appl. Environ. Microb.* 71 (2005) 5523–5531.
- [19] D.B. Bechtel, L.A. Bulla, Electron microscope study of sporulation and parasporal crystal formation in *Bacillus thuringiensis*, *J. Bacteriol.* 127 (1976) 1472–1481.
- [20] Nanoprobes, Nanogold[®] Gold-Streptavidin Conjugate, 2000.
- [21] G. Wolf, J.G. Crespo, M.A.M. Reis, Optical and spectroscopic methods for biofilm examination and monitoring, *Rev. Environ. Sci. Biotechnol.* 1 (2002) 227–251.